Int. J. Heat Mass Transfer. Vol. 35, No. 6, pp. 1385–1396, 1992
Printed in Great Britain

0017–9310/92 $5.00 + 0.00
Pergamon Press Ltd

The influence of capillary hysteresis effects on the humidity and heat coupled transfer in a non-saturated porous medium

C. H. A. MOLENDA, P. CRAUSSE and D. LEMARCHAND
Institut de Mécanique des Fluides, Avenue du Prof. Camille Soula, 31400 Toulouse Cedex, France

(*Received* 18 *March* 1991 *and in final form* 3 *July* 1991)

Abstract—Taking into account the capillary hysteresis effects a mathematical model for mass and heat coupled transfers in non-saturated porous media is used for the numerical simulation of the transfer processes in a closed sand cell and in a cellular concrete wall. The influence of the capillary hysteresis and of the value $(\partial\psi/\partial T)_\omega$ are brought to the fore.

1. INTRODUCTION

THE COUPLED phenomena of mass and energy transfers in non-saturated porous media under the influence of weak thermal gradients are important for diverse natural or industrial processes: the heat and humidity exchanges between the soil and/or building walls and atmosphere, the different drying processes, the thermal insulation, etc.

In spite of the great amount of studies relative to this subject which have been realized during the past three decades, the bibliography shows the lack of analysis on the influence of mass transport properties hysteresis in thermomigration processes. Among these transport properties, the relation between the suction (moisture potential) and conductivity–water content are the most influential. This is due to three factors:

(i) The frequent incapacity in the experimental results analysis to separate the effects due to hysteresis and other causes, for instance heterogeneity, anisotropy and porous medium compressibility, poor control of the interaction between porous medium and environment (boundary conditions), misappreciation of the porous medium initial conditions and hydraulic history.

(ii) The difficulties in determining experimentally the hysteretical relation ψ–ω–T. Besides the necessity of obtaining the principal hysteresis cycle, and sometimes drainage and wetting primary curves according to the hysteresis model that has been used, knowing what influence the temperature has on ψ, at a given water content, requires delicate experimental procedures.

(iii) The most widely used mathematical model of heat and mass transfer in non-saturated porous media, the de Vries [1] model, considers the thermal and water content gradients as driving forces for the transfers. In consequence, among other restrictions [2], the hysteresis in the relation ψ–ω is not taken into account.

The poor knowledge concerning the influence of the ψ–ω hysteresis in thermomigration contrasts with the results obtained in isothermal situations. The non-existence of liquid or vapor transfers due to thermal gradients and the possibility of neglecting the phase changing processes and thermal influence on the hysteretical relation ψ–ω allows a less complicated analysis in this case. Several studies [3–8] have shown the importance of hysteretical effects in the water content distribution in different isothermal situations. The results demonstrate the necessity for a research effort on the consequences of hysteresis in non-isothermal problems.

In this work, we present a mathematical model of mass and energy coupled transfers in a non-saturated porous medium, which takes into account the relation ψ–ω–T hysteresis. This mathematical model is used for the numerical simulation of a thermomigration process in a cell containing sand. After having compared this simulation with the experimental results, the numerical code is used for the prediction of humidity, suction and temperature evolution in a cellular concrete wall.

2. MATHEMATICAL FORMULATION

The hysteresis between ψ and ω prevents the conversion of suction gradient into water content gradient for mass flux determination, as done by Philip and de Vries [9] in their pioneer work. Taking into account this restriction, Milly [10] transformed the equations proposed by de Vries [1] into equations in which the independent variables are suction ψ and temperature T, instead of temperature and water content. The mathematical model proposed in the present work differs from the model presented by Milly in some aspects, dealt with further on.

Obtaining the macroscopic equations which govern the heat and mass transfers in a thermomigration process has been intuitively realized by modeling the

NOMENCLATURE

a	volumetric gas content
a_k	volumetric gas content below which liquid continuity begins
B_T	coefficient of thermal volume expansion of water
C_i	specific heat of phase i
C^*	specific heat of porous medium
D	diffusion coefficient of water vapor in air
D_{Tv}	transport coefficient for vapor flux due to thermal gradient
$D_{\psi v}$	transport coefficient for vapor flux due to ψ gradient
g	acceleration of gravity
h	enthalpy
J_{lc}	capillary-liquid flux
J_{lg}	gravity-liquid flux
J_q	conduction heat flux
J_v	vapor flux
k	unit vector in the positive z direction
K	hydraulic conductivity
L	latent heat of evaporation
M	molar mass of water
P	pressure
P_h	hydrostatic pressure
R	universal gas constant
t	time
T	temperature
V	volumetric trapped air content.

Greek symbols

α	tortuosity
ε	porosity
θ_l	volumetric liquid content
λ	thermal conductivity
λ_a	air thermal conductivity
λ_{ve}	effective vapor thermal conductivity
ρ	density
ρ_0	nominal density of the porous medium
τ	relaxation time
φ	relative humidity
ψ	moisture potential or suction
ω_l	liquid content $\cong$ moisture content
ω_v	vapor content.

Subscripts

0	initial value or nominal value
a	air
l	liquid
q	heat
s	solid
v	vapor
vs	vapor saturation.

porous medium as a multiphase continuum and assuming the following:

the solid phase which constitutes the porous medium is rigid and isotropic in a macroscopic sense;

the gaseous phase total pressure is uniform and constant;

thermodynamic equilibrium between the phases within the porous medium;

there are no chemical reactions between the solid phase and the liquid and gaseous phases;

heat transfers by radiation are negligible;

dissipation effects are negligible in the flow;

the heat of wetting is neglected.

The equations used are the equation of conservation of fluid liquid and vapor phases (1), the equation of energy conservation (2), and the relation between ψ, ω and T, which depends on the porous medium hydraulic history (3).

$$\frac{\partial}{\partial t}[\rho_0(\omega_l\omega_v)] = -\nabla\cdot(J_{lc}+J_{lg}+J_v) \tag{1}$$

$$\frac{\partial}{\partial t}[\rho_0(h_s+h_l\omega_l+h_v\omega_v)] = -\nabla\cdot[J_q+h_l(J_{lc}+J_{lg})+h_vJ_v] \tag{2}$$

$$\omega_l = \omega_l[\psi(t'), t' \leqslant t, T]. \tag{3}$$

The use of Darcy's law (4) to determine the capillary liquid flux J_{lc} has the same drawback as Fourier's law, which when used in heat transfers supposes an infinite speed propagation of thermal perturbations [11, 12]. To avoid this problem the solution usually adopted uses a relaxation time for the heat flux. This time, of the order of 10^{-11} s, 10^{-10} s and 10^{-9} s for solid, liquid and gas respectively, would be negligible for problems normally encountered in practice. Concerning the capillary liquid flux, according to Luikov [12], the relaxation time would be of the order of 10^{-4} s. In this work, the use of a relaxation time τ, equation (5), is motivated by the fact that water content depends on the hydraulic history as well as the actual suction. However, situations in which deviations of hydraulic history due to infinite propagation speed of moisture perturbations are important still remain to be established

$$J_{lc} = -\rho_l K\nabla\psi \tag{4}$$

$$\tau\frac{\partial J_{lc}}{\partial t}+J_{lc} = -\rho_l K\nabla\psi. \tag{5}$$

The liquid flux due to the force of gravity is determined by

$$J_{lg} = -\rho_l Kk. \tag{6}$$

The determination of the vapor flux J_v through a porous medium is realized in the frame of constant total pressure by considering the mixture of water vapor plus air as an ideal mixture and neglecting thermodiffusion [9]

$$J_v = -\alpha a D \frac{P}{P-P_v}\frac{M}{RT}\nabla P_v \tag{7}$$

$$P_v = P_{vs}\exp(\psi Mg/RT) = P_{vs}\varphi. \tag{8}$$

The consideration of local thermodynamic equilibrium between liquid and vapor phases allows the use of Kelvin's equation (8) to obtain an expression for vapor flux in terms of suction and temperature gradients

$$J_v = -\alpha a D \frac{P}{P-P_v}\left(\frac{M}{RT}\right)^2 P_{vs} g\varphi\nabla\psi$$

$$-\alpha a D \frac{P}{P-P_v}\frac{M}{RT}\varphi P_{vs}\left(\frac{1}{P_{vs}}\frac{dP_{vs}}{dT} - \frac{\psi Mg}{RT^2}\right)\nabla T. \tag{9}$$

In the second term of the right-hand side of equation (9), Jury and Letey [13] proposed some correction factors to consider the differences of thermal gradients in the gaseous phase in relation to the porous medium thermal gradient, as well as the vapor path decrease due to the liquid islands. In spite of the lack of a rigorous theoretical justification, using these correction factors, instead of αa, seems to improve the concordance with experimental results. Therefore, these correction factors have been adopted here

$$J_v = -\alpha a D \frac{P}{P-P_v}\left(\frac{M}{RT}\right)^2 P_{vs} g\varphi\nabla\psi - (a+\theta_l g(a))\eta\Gamma D$$

$$\times\frac{P}{P-P_v}\frac{M}{RT}\varphi P_{vs}\left(\frac{1}{P_{vs}}\frac{dP_{vs}}{dT} - \frac{\psi Mg}{RT^2}\right)\nabla T \tag{10}$$

$$\eta = \frac{(\nabla T)_a}{\nabla T} = \frac{(\nabla T)_a}{a(\nabla T)_a + \theta_l(\nabla T)_l + (1-a-\theta_l)(\nabla T)_s} \tag{11}$$

$$\Gamma = \left[\frac{a+\theta_l g(a)}{a+\theta_l(\lambda_{ve}/\lambda_l)g(a)}\right]^2 \tag{12}$$

$$\left.\begin{aligned} g(a) &= 1 \quad a > a_k \\ g(a) &= a/a_k \quad a < a_k \end{aligned}\right\}. \tag{13}$$

η is the ratio between the thermal gradient in the gaseous phase and the thermal gradient in the porous medium; $(\nabla T)_a$, $(\nabla T)_l$ and $(\nabla T)_s$ are the average thermal gradients in, respectively, the gaseous, liquid and solid phases. de Vries [14] has given an estimation method for the average thermal gradients in the different phases. a_k is the volumetric content of the gaseous phase for which the liquid continuity starts. λ_{ve} is the effective thermal conductivity in the gaseous phase at pore scale. Besides the air thermal conductivity it considers a term due to latent heat transfer by the vapor flux

$$\lambda_{ve} = \lambda_a + LD\frac{P}{P-P_v}\frac{M}{RT}\frac{dP_{vs}}{dT}. \tag{14}$$

The conduction heat flux J_q is determined by Fourier's law

$$J_q = -\lambda\nabla T. \tag{15}$$

Equations (1)–(3) make up a system of three equations and four unknowns, ω_l, ω_v, ψ and T. The variable ω_v is eliminated by using equation (17) obtained with the help of the ideal gas law, Kelvin's law (8) and relation (16)

$$\omega_v = (\varepsilon-\theta_l)\frac{\rho_v}{\rho_0} \tag{16}$$

$$\frac{\partial\omega_v}{\partial t} = -A\frac{\partial\omega_l}{\partial t} + B\frac{\partial\psi}{\partial t} + C\frac{\partial T}{\partial t} \tag{17}$$

$$A = \frac{MP_{vs}\varphi}{RT\rho_l} \tag{18}$$

$$B = agP_{vs}\left(\frac{M}{RT}\right)^2\frac{\varphi}{\rho_0} \tag{19}$$

$$C = \frac{aMP_{vs}\varphi}{RT\rho_0}\left[\frac{1}{P_{vs}}\frac{dP_{vs}}{dT} - \frac{\psi Mg}{(RT)^2} - \frac{1}{T}\right]. \tag{20}$$

The theoretical model to be solved is established with the help of equation (17) and by neglecting the influence of temperature upon the specific heat of each phase

$$(1-A)\frac{\partial\omega_l}{\partial t} + B\frac{\partial\psi}{\partial t} + C\frac{\partial T}{\partial t} = -\frac{1}{\rho_0}\nabla\cdot(J_{lc}+J_{lg}+J_v) \tag{21}$$

$$(h_l - Ah_v)\frac{\partial\omega_l}{\partial t} + Bh_v\frac{\partial\psi}{\partial t} + (C^* + h_v C)\frac{\partial T}{\partial t}$$

$$= -\frac{1}{\rho_0}\nabla\cdot[J_q + h_l(J_{lc}+J_{lg}) + h_v J_v] \tag{22}$$

$$\omega_l = \omega_l[\psi(t'), t' \leqslant t, T] \tag{3}$$

$$\tau\frac{\partial J_{lc}}{\partial t} + J_{lc} = -\rho_l K\nabla\psi \tag{5}$$

$$J_{lg} = -\rho_l K k \tag{6}$$

$$J_v = -D_{\psi v}\nabla\psi - D_{Tv}\nabla T \tag{23}$$

$$J_q = -\lambda\nabla T \tag{15}$$

$$D_{\phi v} = \alpha a D\frac{P}{P-P_v}\left(\frac{M}{RT}\right)^2 P_{vs} g\varphi \tag{24}$$

$$D_{lJv} = (a+\theta_l g(a))\eta\Gamma D\frac{P}{P-P_v}\frac{M}{RT}\varphi P_{vs}$$

$$\times\left(\frac{1}{P_{vs}}\frac{dP_{vs}}{dT} - \frac{\psi Mg}{RT^2}\right) \tag{25}$$

$$C^* = C_s + \omega_l C_l + \omega_v C_v \tag{26}$$

in which C_i (i = s, l, v) are the specific heats of the i phases.

This mathematical model differs from the model presented by Milly [10] in the following aspects:

the consideration of a relaxation time for the capillary liquid flux;

using the correction factors proposed by Jury and Letey [13] for the vapor transport coefficient due to the thermal gradient;

the non-consideration of the heat of wetting, negligible in most of the applications.

Moreover Milly's model consists of two differential equations for ψ and T where the transport coefficients depend on ψ, T and the hydraulic history of the porous medium. In this work the terms in ω_l are maintained and the hysteretical relation ψ–ω_l–T enters the model as a third equation. This shows the possibility of considering the transport coefficients as dependent on ψ–ω–T, instead of on ψ–T and hydraulic history.

3. MODELIZATION OF ψ–ω_l–T AND K–ω_l–T RELATIONS

The choice of hysteresis model is a function of the quantity of experimental data necessary on model calibration, the easiness of use and, of course, the quality of results. Among the numerous existing models, Mualem's model II [15] and Mualem and Dagan's model III [16] seem to be the most satisfactory. In this work Mualem's model II was chosen because it requires as experimental data only the main hysteresis cycle. However, it is not so precise as model III, in particular concerning porous media which have a great part of their hysteresis loop in the range of air-intry-value.

Mualem's model II provides simple expressions for curve simulation inside the hysteresis cycle. During a wetting, after a series of drainage and wetting processes, the value of Ω, defined as the difference between the water content and the residual water content $\Omega = \omega_l - \omega_{l\min}$, is given by

$$\Omega\begin{pmatrix}\psi_1 \dots \psi \\ \psi_{\min}\ \psi_2 \dots \psi_N\end{pmatrix} = \Omega_w(\psi) + [\Omega_w(\psi_{N-1}) - \Omega(\psi)]\frac{\Omega_d(\psi_N) - \Omega_w(\psi_N)}{\Omega_u - \Omega_w(\psi_N)} + \sum_{j=1}^{(N/2)-1} [\Omega_w(\psi_{2j-1}) - \Omega_w(\psi_{2j+1})] \times \frac{\Omega_d(\psi_{2j}) - \Omega_w(\psi_{2j})}{\Omega_u - \Omega_w(\psi_{2j})}. \quad (27)$$

The left-hand side of this equation indicates that the process consists first in an increase of $\psi_{\min}$ to ψ_1 (wetting), and then in a decrease of ψ_1 to ψ_2 (drainage), increase of ψ_2 to ψ_3 and so on. Ω_w indicates the $\Omega(\psi)$ value read on the principal wetting curve, $\Omega_d(\psi)$ the value read on the principal drainage curve and Ω_u is the maximum water content.

The Ω value during a drainage is given by

$$\Omega\begin{pmatrix}\psi_1 \dots \psi_N \\ \psi_{\min}\ \psi_2 \dots \psi\end{pmatrix} = \Omega_w(\psi) + [\Omega_w(\psi_N) - \Omega_w(\psi)]\frac{\Omega_d(\psi) - \Omega_w(\psi)}{\Omega_u - \Omega_w(\psi)} + \sum_{j=1}^{(N-1)/2} [\Omega_w(\psi_{2j-1}) - \Omega_w(\psi_{2j+1})] \times \frac{\Omega_d(\psi_{2j}) - \Omega_w(\psi_{2j})}{\Omega_u - \Omega_w(\psi_{2j})}. \quad (28)$$

The influence of the temperature on the relation $\psi - \omega_l$ is still a difficult point to study because of delicate experimental processes. Some studies [17–19] obtained a good concordance between the experimental results and the theory which considers that the thermal effects on suction ψ would only be due to variations of the tension surface σ with the temperature

$$\left(\frac{\partial\psi}{\partial T}\right)_{\omega_l} = \frac{\psi}{\sigma}\frac{d\sigma}{dT} = \gamma\psi \quad (29)$$

in which γ is called the superficial tension coefficient. However, in these works, $(\partial\psi/\partial T)_{\omega_l}$ was determined by using different $\psi = \psi(\omega_l)$ isothermal curves, which neglect the volume variation of the solid, liquid and trapped air phases. Other works [20, 21] determined $(\partial\psi/\partial T)_{\omega_l}$ by varying the temperature of porous media with constant water content, though this process is a delicate one. These works obtained values of $(\partial\psi/\partial T)_{\omega_l}$ dependent on the water content and 5–100 times greater than the values given by equation (29). Peck [22] included in his theoretical study the water and trapped air thermal expansion effects, having obtained the following relation:

$$\left(\frac{\partial\psi}{\partial T}\right)_{\omega_l} = \gamma\psi + \frac{B_T\theta_l T P_h + V(P_h - \gamma T\psi)}{T\left(P_h\frac{\partial\theta_l}{\partial\psi} - V\right)} \quad (30)$$

in which B_T is the water thermal expansion coefficient, P_h is the water hydrostatic pressure (ψ plus atmospheric pressure) and V is the trapped air volume. This equation provides values greater than those obtained by only considering the effects due to superficial tension and shows the $(\partial\psi/\partial T)_{\omega_l}$ dependence on the porous medium hydraulic history (dependence on water content, suction, temperature and trapped air volume). In this work, as equation (30) requires knowledge of the trapped air volume, the following relation, in which $n \geqslant 1$, has been adopted

$$\left(\frac{\partial\psi}{\partial T}\right)_{\omega_l} = n\gamma\psi. \quad (31)$$

The comparison between the simulations with different values of n and the experimental results should allow the determination of the adapted value of n. The use of this law for every water content for the whole hysteresis cycle at every temperature is a simplification, the extent of which can only be shown by precise experimental results.

The determination of the K–ω_l–T relation is also delicate in so far as thermomigration problems are concerned. The K–ω_l hysteresis (due to that for the same water content the filled pores radii distribution is different according to whether the porous medium was subjected to drainage or to wetting) is normally negligible in many practical situations. On the other hand, the experimental results relative to the thermal influence on the hydraulic conductivity are con-

troversial [18, 23–25]. In this work we adopt a formula according to which this influence acts through the water viscosity, in accordance with the equation below

$$K = \frac{kg}{v} \tag{32}$$

where k is the effective medium permeability, considered as independent from temperature, and v is the cinematic viscosity of the water.

4. NUMERICAL FORMULATION

The method used to solve the equation set proposed in this work in bidimensional fields has been the classical finite volume method, fully implicit, presented by Patankar [26]. Concerning the capillary liquid flux, the existence of a relaxation time requires a modification of the discretization in time. The resolution of equation (5), considering $\rho_l K \nabla\psi$ as constant, will be

$$J_{lc} = J_{lc0} \exp\left(\frac{-t}{\tau}\right) - \rho_l K \nabla\psi \left[1 - \exp\left(\frac{-t}{\tau}\right)\right] \tag{33}$$

in which J_{lc0} is the initial flux. In a time interval Δt the flux is determined by

$$\int_{\Delta t} J_{lc}\, dt = J_{lc}^{n}\tau\left[1 - \exp\left(\frac{-\Delta t}{\tau}\right)\right] - \rho_l K \nabla\psi^{n+1}\left\{\Delta t - \tau\left[1 - \exp\left(\frac{-\Delta t}{\tau}\right)\right]\right\}. \tag{34}$$

The superscript n indicates values at the initial instant of a time interval and $n+1$ at its end. The discretization shown in equation (34) is also valid for the other flux, considering a relaxation time of zero.

The equation set resolution is realized in an interactive way by using a line-by-line scheme for each equation [26]. First of all the energy conservation equation, then the mass conservation equation and finally, the water content determination by Mualem's model II are considered. After a certain number of interactions, the water content of each finite volume is compared to the water content of the previous time step to evaluate whether there is wetting or drainage and to determine the hydraulic history reverse points; then the transport coefficients depending on ψ, ω and temperature T are actualized. A detailed presentation of the solution method can be found in ref. [27].

5. APPLICATION

The theory developed above has been applied to the heat and mass coupled transfer analysis in the following two physical configurations: a closed cell containing sand and a cellular concrete wall.

5.1. *Closed system*

An experimental study was realized on a non-saturated porous medium sample (quartzic sand geometrically characterized by $d_{10} = 140$ μm and $d_{60} = 240$ μm), set up in a 350 mm long and 60 mm diameter cylindrical cell with a horizontal axis (Fig. 1). The cells ends, $x = 0$ and L, are closed by a thermostatted water circulation. The side surface is thermally isolated by a guard device and drilled with a few 1 mm diameter aerations which permit us to keep a uniform gaseous phase pressure, equal to the atmospheric pressure. Before filling the cell, the sand is mixed with an adequate water quantity so as to reach the desired water content $\omega_0 = 0.11$ kg kg^{-1}. The cell is filled in by compression and settled in a thermal medium at $T_0 = 20$°C.

After 48 h rest the thermal gradient is imposed: 54°C at one cell base and 20°C at the other. A series of cells was subjected to this gradient for 6 days, another for 8 days, and a third one for 13 days. The water content distribution was determined by cutting into 1 cm thick slices weighing, drying in an oven then weighing again.

The results obtained with the different series of cells showed no greater differences than experimental errors. Consequently, to compare the numerical results we use a least square curve according to Fig. 2, in which the left side is subjected to 54°C and the right one to 20°C.

The numerical simulation has been realized in a 350×60 mm rectangular field divided into 210 volumes. The necessary experimental data for simulation, the hysteresis cycle (Fig. 3) and the hydraulic conductivity (Fig. 4) were obtained in ref. [6]. The thermal conductivity used was determined by Crausse [18, 28], by using a sand of slightly different porosity. The initial values adopted were: $\omega_0 = 0.11$ kg kg^{-1}, $T_0 = 20$°C, $J_{lc0} = 0$ kg m^{-2} s^{-1}. Considering that the

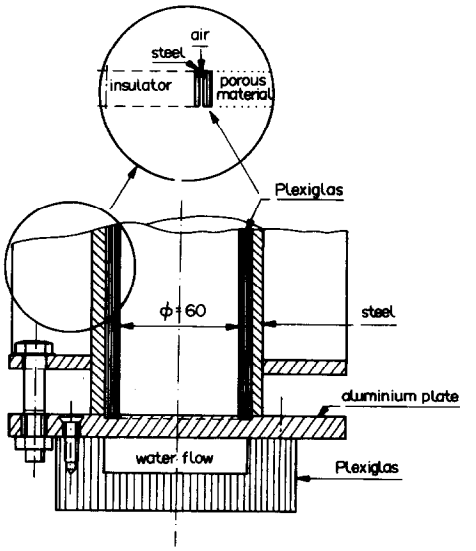

FIG. 1. Experiment cell.

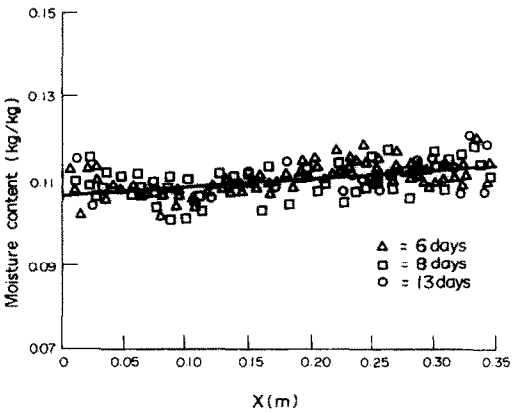

FIG. 2. Experimental results.

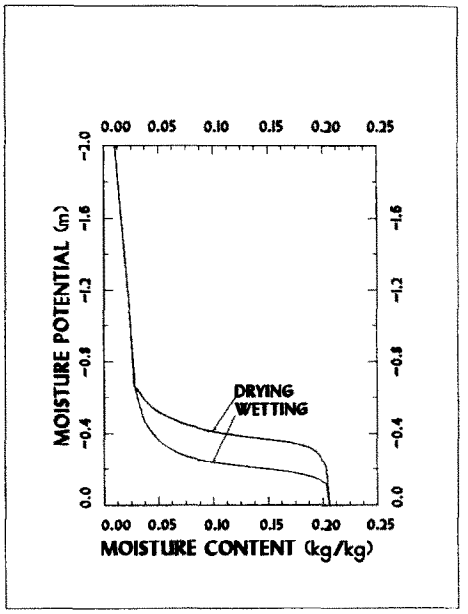

FIG. 3. Hysteresis loop of the sand.

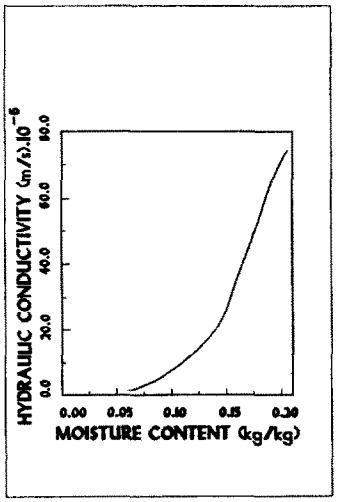

FIG. 4. Hydraulic conductivity of the sand.

initial value of moisture potential ψ_0 as well as the experimental hydraulic history were unknown, different values of ψ_0 were tried in drainage and in wetting. At the horizontal boundaries the mass and energy flux conditions are nil. At the vertical boundaries, corresponding to the cylindrical experimental cell basis, the conditions are nil mass flux and fixed temperature.

As for the boundary conditions presently concerned, time independent, no difference has been observed between the results obtained by using a relaxation time τ for the capillary liquid flux of the order of 10^{-4} s and a relaxation time of zero.

Figures 5 and 6 show the simulation results for the permanent state regime (reached in 4 days) without considering the hysteresis; $n = 3$ corresponds to the n value used in equation (31). In order to compare the experimental and numerical results, we have realized vertical averages. These results are shown in Figs. 7 and 8. For the simulation which takes the hysteresis into account, we used an initial suction value situated between the drainage curve value and the wetting

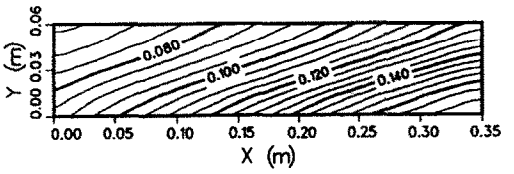

FIG. 5. Moisture content distribution (drying curve only, $n = 3$).

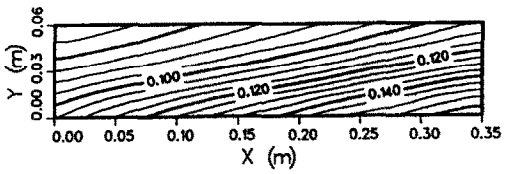

FIG. 6. Moisture content distribution (wetting curve only, $n = 3$).

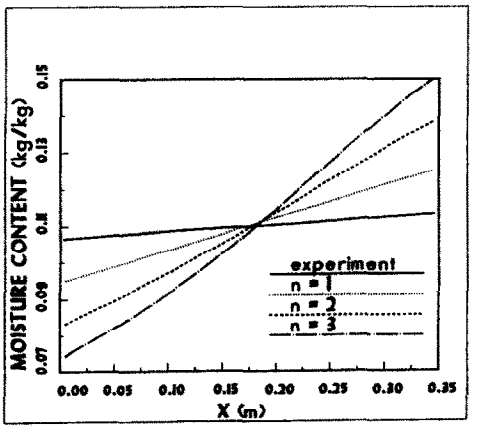

FIG. 7. Simulation results (drying curve only).

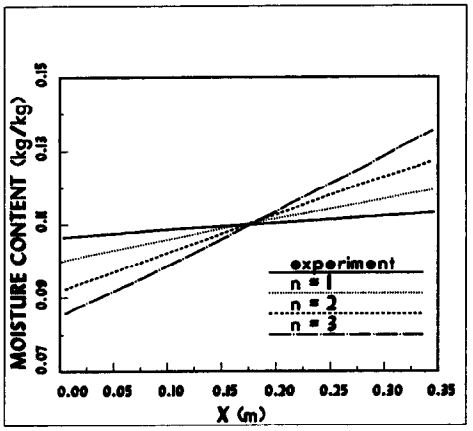

FIG. 8. Simulation results (wetting curve only).

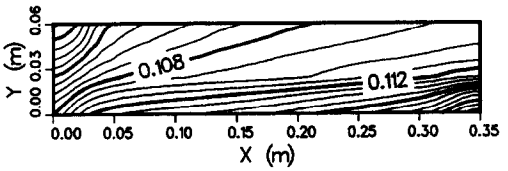

FIG. 9. Moisture content distribution (with hysteresis, $n = 3$).

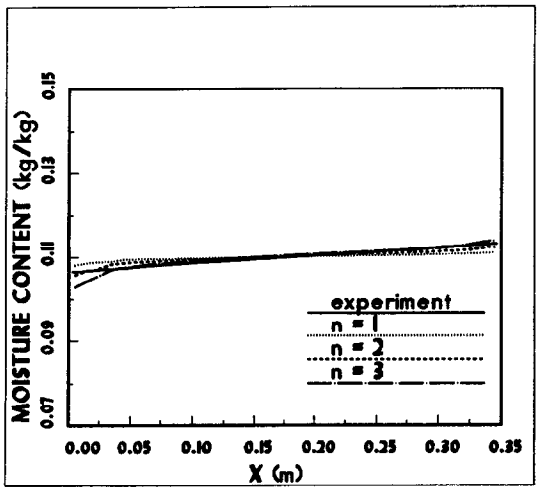

FIG. 10. Comparison between experiment and simulation with hysteresis.

curve value, $\psi_0 = -0.313$ m, and the initial hydraulic history: wetting with the last reverse point $\omega = 0.01$ kg kg^{-1} and $\psi = -2.00$ m (Figs. 9 and 10). The results obtained with some other reverse points are no different. Figure 11 shows the thermal distribution obtained by simulations with and without hysteresis.

These results show that in the case of this porous medium, and with the considered boundary conditions, neglecting the hysteresis leads to considerable mistakes in the humidity distribution prediction, in particular for high values of n. However, because of the weak thermal conductivity variation, in the considered water content range, the hysteresis does not seem to influence the thermal profile.

5.2. *Open system*

In this example, numerical simulations concerning a cellular concrete sample of density $\rho_0 = 450$ kg m^{-3} are realized. The hysteresis cycle used (Fig. 12) is based on the results obtained with the mercury porosimeter and a simplified version of Mualem's model II [15]. This simplification consists of considering the pore openings radii distribution being equal to the pore radii distribution. The hydraulic and thermal conductivity were respectively obtained in refs. [29, 30].

The physical model analyzed is shown in Fig. 13 where φ is the relative humidity. Due to the slight influence of gravity for the initial water content adopted, $\omega_0 = 0.20$, the simulations are realized in a unidimensional domain divided into 40 volumes. Concerning this problem the relaxation time influence tests have not been done. Thus the τ value used is 0.

Figures 14–19 show some results obtained by simulation with or without hysteresis. The influence of hys-

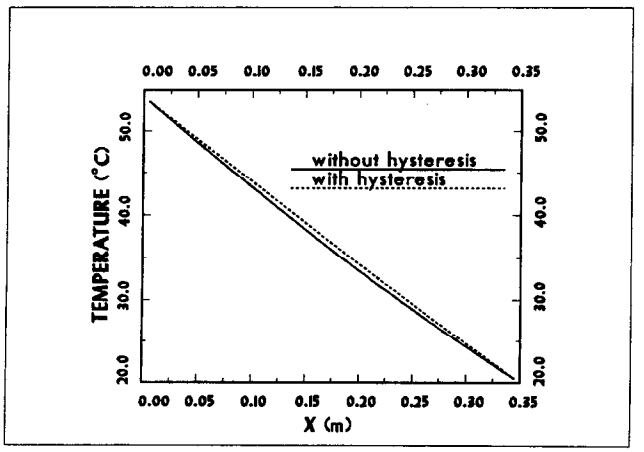

FIG. 11. The temperature distributions.

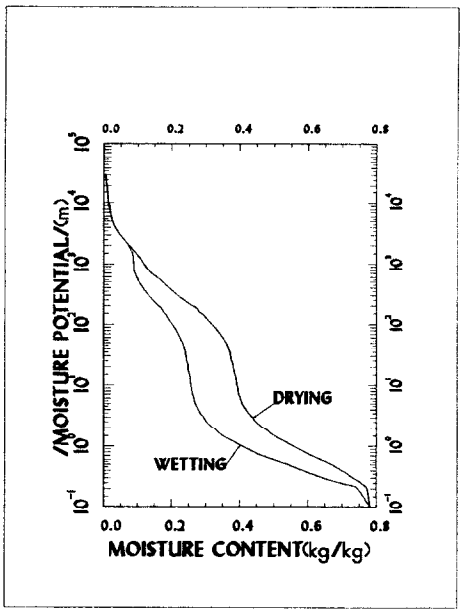

FIG. 12. Hysteresis loop of the cellular concrete.

teresis is shown in Figs. 20–22, and the influence of n value can be seen in Figs. 23 and 24. The temperature profiles obtained from the different numerical simulations did not present important differences. The thermal steady-state profile is obtained after about 24 h (Fig. 25).

The slight influence of hysteresis observed in this example can possibly be explained by the hysteresis cycle used, which needs experimental confirmation. However, the results shown in Figs. 20–22 lead to the conclusion that hysteresis favors the cellular concrete wall draining in a certain period of time during the process.

6. CONCLUSION

The use of the mathematical model shown in this work for the numerical simulation of mass and heat coupled transfers in a porous medium has allowed the analysis of the capillary hysteresis influence effects, the capillary liquid flux relaxation time and the $(\partial\psi/\partial T)_\omega$ value, in strictly determined physical situations. There is no influence of the relaxation time for the boundary conditions fixed in time. However, in spite of the sim-

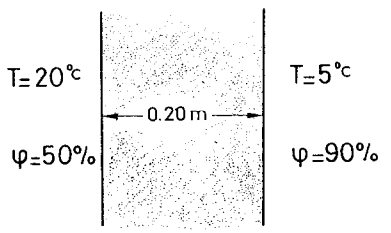

FIG. 13. The physical model.

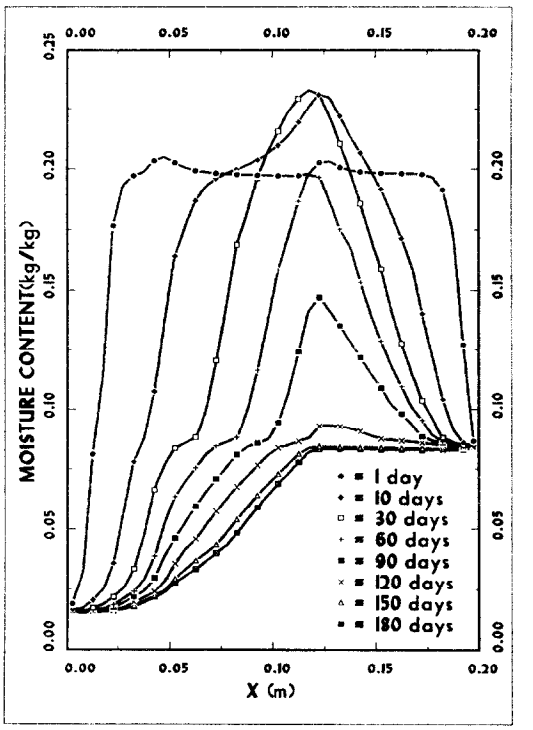

FIG. 14. Simulation results (without hysteresis, $n = 1$).

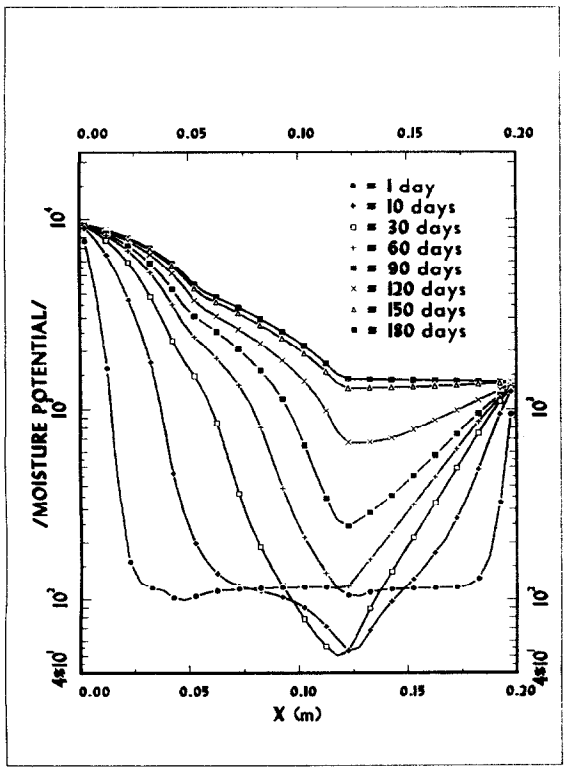

FIG. 15. Simulation without hysteresis, $n = 1$.

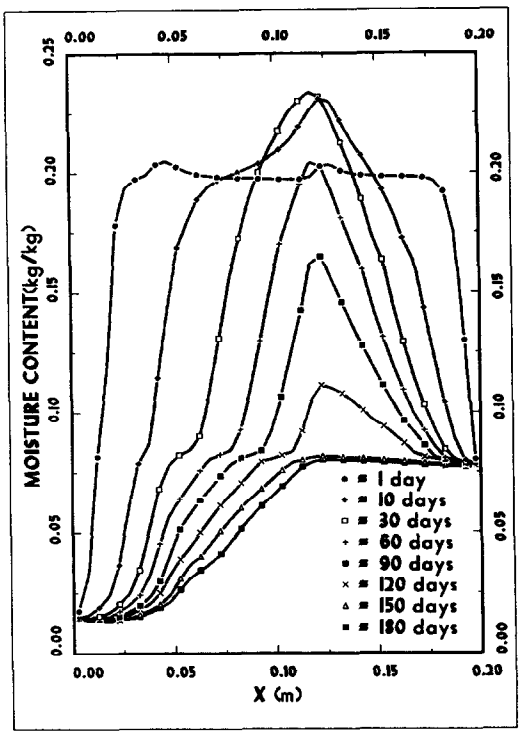

FIG. 16. Simulation without hysteresis, $n = 3$.

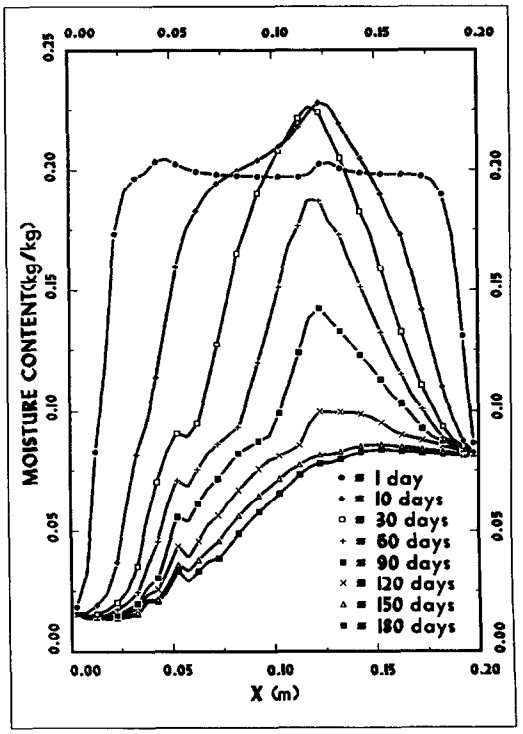

FIG. 18. Simulation with hysteresis, $n = 3$.

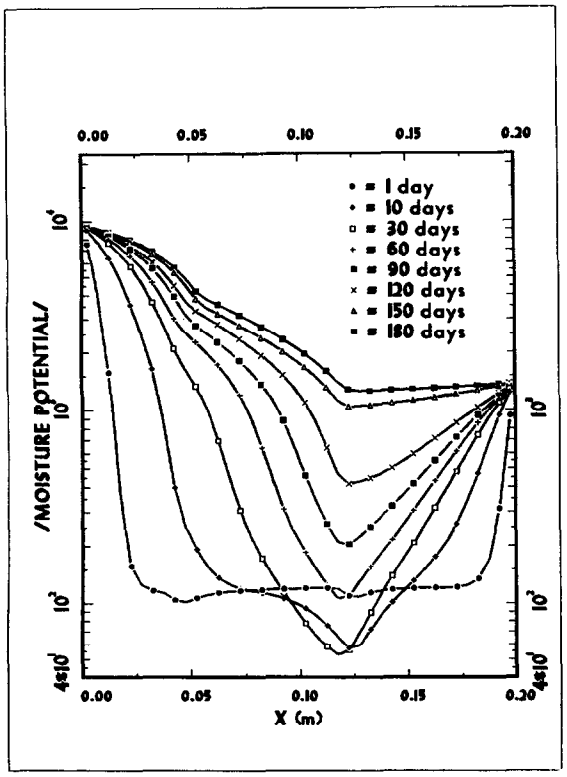

FIG. 17. Simulation without hysteresis, $n = 3$.

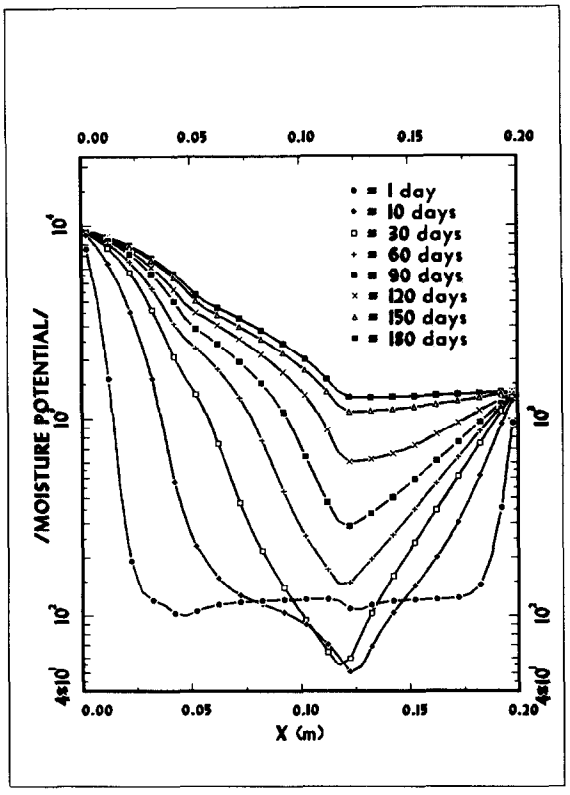

FIG. 19. Simulation with hysteresis, $n = 3$.

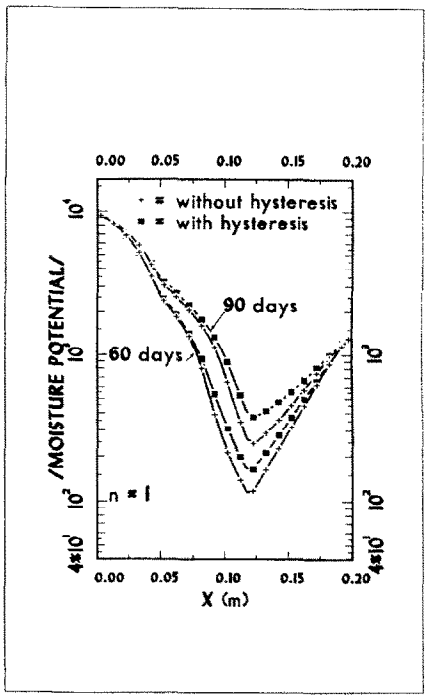

FIG. 20. Comparison between simulations with and without hysteresis, moisture potential.

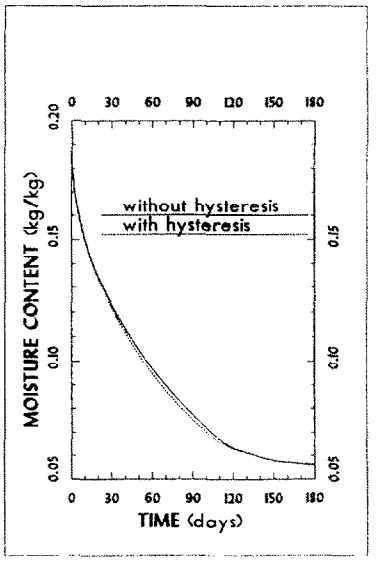

FIG. 22. Comparison between the average moisture contents.

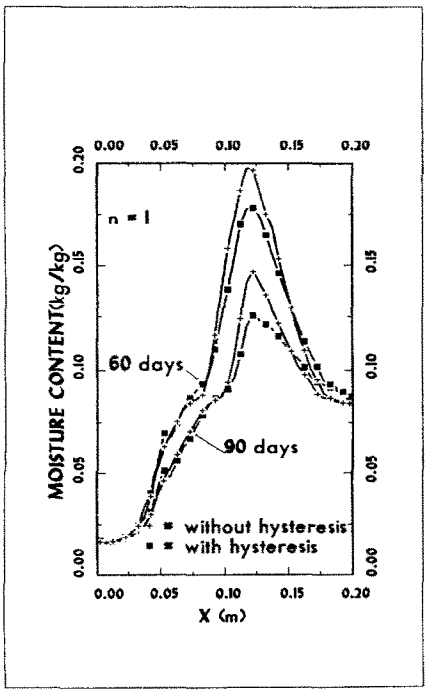

FIG. 21. Comparison between simulations with and without hysteresis, moisture content.

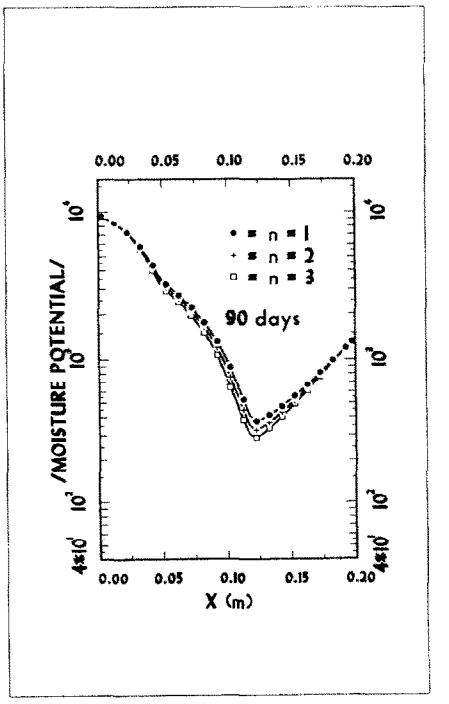

FIG. 23. Simulation with hysteresis, 90 days.

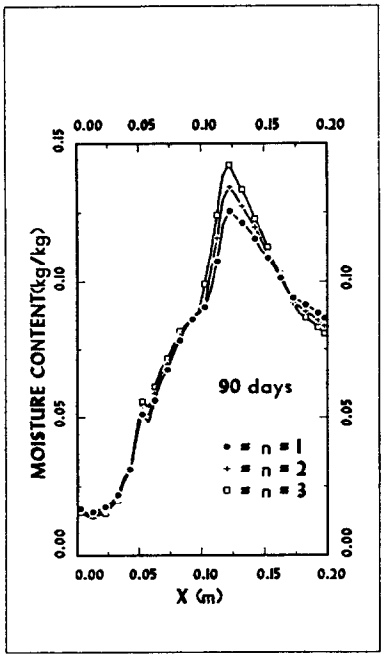

FIG. 24. Simulation with hysteresis.

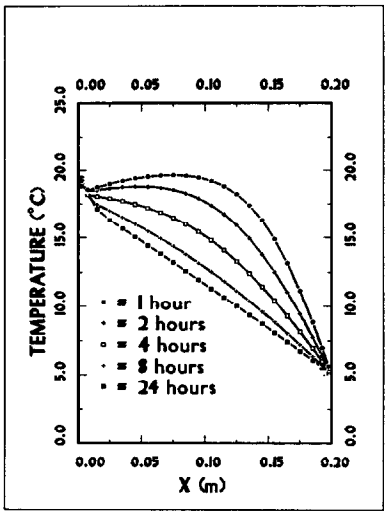

FIG. 25. Evolution of the temperature profile.

plicity of the problems analyzed, the results show the role played by capillary hysteresis and the necessity of knowing the correct value of $(\partial\psi/\partial T)_\omega$.

Acknowledgements—This paper is part of the thesis of the senior author to be submitted to the Institut National Polytechnique de Toulouse, as a partial fulfillment of the requirements of the Doctor degree, and was partly supported by the C.N.R.S.-PIRSEM and SIPOREX-France.

REFERENCES

1. D. A. de Vries, Simultaneous transfer of heat and moisture in porous media, *Trans. Am. Geophys. Un.* **39,** 909–916 (1958).
2. D. A. de Vries, The theory of heat and moisture transfer in porous media revisited, *Int. J. Heat Mass Transfer* **30,** 1343–1350 (1987).
3. J. Rubin, Numerical method for analysing hysteresis affected, post-infiltration redistribution of soil moisture, *Soil Sci. Soc. Am. Proc.* **31,** 13–20 (1967).
4. S. J. Lees and K. K. Watson, The use of a dependent domain model of hysteresis in numerical soil water studies, *Water Resour. Res.* **11,** 943–948 (1975).
5. F. Beese and R. R. van der Ploeg, Influence of hysteresis on moisture flow in undisturbed soil monolith, *Soil Sci. Am. J.* **40,** 480–484 (1976).
6. N. T. Hoa, Ecoulements non permanents dans des massifs de milieux poreux non saturés avec effet d'hystérésis, Thèses doctorat d'etat, I.N.P. Toulouse (1978).
7. J. M. Royer and G. Vachaud, Field determination of hysteresis in soil–water characteristic, *Soil Sci. Am. J.* **39,** 221–223 (1979).
8. A. A. Curtis and K. K. Watson, Hysteresis affected water movement in scale heterogeneous profiles, *Water Resour. Res.* **20,** 719–726 (1984).
9. J. R. Philip and D. A. de Vries, Moisture movement in porous materials under temperature gradients, *Trans. Am. Geophys. Un.* **38,** 222–232 (1957).
10. P. C. D. Milly, Moisture and heat transport in hysteretic, inhomogeneous porous media : a matric head-based formulation and a numerical model, *Water Resour. Res.* **18,** 489–498 (1982).
11. D. D. Joseph and L. Preziosi, Heat waves, *Rev. Mod. Phys.* **61,** 41–73 (1988).
12. A. V. Luikov, Application of irreversible thermodynamics methods to investigation of heat and mass transfer, *Int. J. Heat Mass Transfer* **9,** 139–152 (1966).
13. W. A. Jury and J. Letey Jr., Water movement in soil: reconciliation of theory and experiment, *Soil Sci. Soc. Am. J.* **43,** 823–827 (1979).
14. D. A. de Vries, Het Warmtegeleidingsvermogen van grond, Meded. Landbouwhogeschool Wageningen **52,** 1–73 (1952).
15. Y. Mualem, A conceptual model of hysteresis, *Water Resour. Res.* **10,** 514–520 (1974).
16. Y. Mualem and G. Dagan, A dependent domain model of capillary hysteresis, *Water Resour. Res.* **11,** 452–460 (1975).
17. R. S. Chahal, Effect of temperature and trapped air on matrix suction, *Soil Sci.* **100,** 262–266 (1965).
18. P. Crausse, Etude fondamentale des transferts couplés de chaleur et d'humidité en milieux poreux non saturés, Thése doctorat d'état, I.N.P. Toulouse (1983).
19. J. W. Hopmans and J. H. Dane, Temperature dependence of soil water retention curves, *Soil Sci. Am. J.* **50,** 562–567 (1986).
20. S. A. Taylor and G. L. Stewart, Some thermodynamic properties of soil water, *Soil Sci. Am. Proc.* **24,** 243–247 (1960).
21. W. A. Jury and E. E. Miller, Measurement of the transport coefficients for coupled flow of heat and moisture in a medium sand, *Soil Sci. Soc. Am. Proc.* **38,** 551–557 (1974).
22. A. J. Peck, Change of moisture with temperature and air pressure : theoretical, *Soil Sci.* **89,** 303–310 (1960).
23. W. J. Flocker, M. Yamaguchi and D. R. Nielsen, Capillary conductivity and soil water diffusivity values from vertical soil columns, *Argon J.* **60,** 605–610 (1968).
24. M. Haridasan and R. D. Jensen, Effect of temperature on pressure head-water content relationship and conductivity of two soils, *Soil Sci. Soc. Am. Proc.* **36,** 703–708 (1972).
25. J. Constantz, Temperature dependence of unsaturated

hydraulic conductivity of two soils, *Soil Sci. Soc. Am. J.* **46,** 466–470 (1982).
26. S. V. Patankar, *Numerical Heat Transfer and Fluid Flow*. Hemisphere, New York (1980).
27. C. H. A. Molenda, Influence des effets d'hystérésis sur les phénomènes de transferts couplés de chaleur et masse en milieux poreux, Thèse de doctorat de l'I.N.P.T., Toulouse.
28. P. Crausse, G. Bacon and S. Bories, Etude fondamentale des transferts couplés chaleur-masse en milieu poreux, *Int. J. Heat Mass Transfer* **24,** 991–1004 (1981).
29. C. H. A. Molenda, P. Crausse, J. Cid and D. Lemarchand, Etude des phénomènes de transfert de chaleur et d'humidité en béton cellulaire, Rapport GEMP, IMFT, Toulouse (1990).
30. D. Quenard and H. Salle, Contribution à la caractérisation hygrothermique du béton cellulaire autoclavé, Rapport GM/88-670, CSTB Grenoble (1988).

INFLUENCE DES EFFETS D'HYSTERESIS CAPILLAIRE SUR LE TRANSFERT COUPLE D'HUMIDITE ET DE CHALEUR DANS UN MILIEU POREUX NON SATURE

Résumé—En prenant en compte les effets d'hystérésis capillaire, un modèle mathématique des transferts couplés de masse et de chaleur dans un milieu poreux non saturé est utilisé en vue de la simulation numérique des phénomènes de transfert dans une cellule fermée contenant du sable et dans un mur en béton cellulaire. L'influence de l'hystérésis capillaire et des effets de température $(\partial\psi/\partial T)_\omega$ sont pris en compte simultanément.

DER GEKOPPELTE FEUCHTIGKEITS- UND WÄRMETRANSPORT IN EINEM NICHTGESÄTTIGTEN PORÖSEN MEDIUM UNTER DEM EINFLUS DER KAPILLAREN HYSTERESE

Zusammenfassung—Ein mathematisches Modell des Wärme- und Stofftransports in ungesättigten porösen Medien wird zur numerischen Simulation der Transportvorgänge in einer abgeschlossenen Sandzelle und einer zellförmigen Betonwand angewandt. Dabei wird der kapillare Hysterese-Einfluß berücksichtigt, der zusammen mit dem Wert $(\partial\psi/\partial T)_\omega$ in den Vordergrund gestellt wird.

ВЛИЯНИЕ КАПИЛЛЯРНОГО ГИСТЕРЕЗИСА НА СОВМЕСТНЫЙ ПЕРЕНОС ВЛАГИ И ТЕПЛА В НЕНАСЫЩЕННОЙ ПОРИСТОЙ СРЕДЕ

Аннотация—При помощи математической модели совместного массо- и теплопереноса в ненасыщенных пористых средах с учетом капиллярного гистерезиса численно моделируются процессы переноса в замкнутой ячейке песка в ячеистой бетонной стенке. Исследуется влияние капиллярного гистерезиса и значения $(\partial\psi/\partial T)_\omega$.